Development of a high throughput and low cost model for the study of semi-dry biofilms

Ngozi Amaeze[a,e], Ayorinde Akinbobola[a], Valentine Chukwuemeka[a], Adil Abalkhaila[b], Gordon Ramage[c], Ryan Kean[d], Harry Staines[e], Craig Williams[a], William Mackay[a]

[a]Institute of Healthcare Policy and Practice, School of Health and Life Sciences, University of the West of Scotland, Paisley, Scotland, UK

[b]Department of Human Health, College of Applied Medical Sciences Qassim University, Buraydah, KSA

[c]Oral Sciences Research Group, School of Medicine, Dentistry and Nursing, College of Medical, Veterinary and Life Sciences, University of Glasgow, Glasgow, UK.

[d]Biological and Biomedical Sciences, Glasgow Caledonian University, Glasgow, UK

[e]Sigma Statistical Services, Balmullo, UK

[f]Department of Microbiology, University of Abuja, Nigeria

Correspondence: William Mackay

Institute of Healthcare Policy and Practise, School of Health and Life Sciences, University of the West of Scotland, Paisley, Scotland, UK

w.mackay@uws.ac.uk

Abstract

The persistence of microorganisms as biofilms on dry surfaces resistant to usual terminal cleaning methods may pose an additional risk of transmission of infections. In this study, the Centre for Disease Control (CDC) dry biofilm model (DBM) was adapted into a microtiter plate format (Model 1) and replicated to create a novel in vitro model that replicates conditions commonly encountered in the healthcare environment (Model 2). Biofilms of *S. aureus* grown in the two models were comparable to the biofilms of the CDC DBM in terms of recovered $\log_{10}$ CFU/well. Assessment of antimicrobial tolerance of biofilms grown in the two models showed Model 2 a better model for biofilm formation. Confirmation of biofilms phenotype with an extracellular matrix deficient *S. aureus* suggested stress tolerance through a non-matrix defined mechanism in organisms. This study highlights the importance of conditions maintained in bacterial growth as they affect biofilm phenotype and behaviour.

Running title: High throughput semi-dry biofilm model

Keywords: Biofilms, Biofilm primed aggregates, environment, *Staphylococcus aureus*, persistence

Introduction

It is estimated that 3.2 million people in Europe acquire healthcare associated infections (HAIs) each year, with an average prevalence of 6% in acute hospitals (Kritsotakis et al. 2017). While the prevalence of HAIs has reduced over recent years, there is still a need to better understand the contribution of the healthcare environment to HAI, in particular how microorganisms persist and transfer within the healthcare environment.

Infection prevention control strategies have been developed to prevent the persistence of pathogens in the hospital environment and subsequent onward transmission of infection (Lei et al. 2017). Terminal cleaning, for example, is undertaken after patient discharge to eliminate the risk of transfer of infection to the next occupant of the room. However, recent studies have shown that microorganisms may survive terminal cleaning and it has been suggested that they are present in the form of biofilms (Hu et al. 2015; Almatroudi et al. 2016).

Biofilms are the preferred mode of existence for microorganisms in the environment, consisting of attached microbial cells organised into microcolonies that are surrounded with extracellular polymeric substances (EPS) also known as extracellular matrix (ECM) (Costerton JW et al. 1995; Arampatzi et al. 2011; Richmond et al. 2016). The biofilm phenotype confers unique characteristics making biofilms more tolerant to stressors, including antimicrobials, heat, nutrient deprivation, and desiccation, when compared to their planktonic counterparts (Donlan Rodney M 2002; Høiby Niels et al. 2010).

In a study of a terminally cleaned intensive care unit (ICU) in Australia where destructive sampling was used, it was reported that microorganisms were surviving in the form of biofilms on a variety of dry surfaces, including curtains, mattresses and pillows (Vickery et al. 2012). In the United Kingdom, dry biofilms containing bacterial pathogens were found on 61 terminally cleaned items received from 3 different UK hospitals (Ledwoch et al. 2018). *Staphylococcus aureus,* a commensal that becomes an opportunistic pathogen in elderly, sick and immunocompromised patients, was frequently isolated in these studies (Chowdhury et al. 2018). Following these observations, the same group devised a method of growing *S. aureus* biofilms that were similar both in terms of composition and gross morphology to those isolated from dry surfaces in the ICU (Almatroudi et al. 2015). This methodology involved

shaking the cultures alongside extended periods of dehydration at 66% relative humidity (RH), interspersed with periods of hydration at 4, 7and 9 days. This was different to most studies on biofilms in the built environment that typically maintain conditions of high nutrient and moisture (Kostaki et al. 2012; Muazu et al. 2017; Gomes et al. 2018).

The primary aim of this study was to adapt the original CDC semi-dry biofilm bioreactor model into a cost-effective and easily reproducible high throughput semi-dry biofilm model that is applicable to the healthcare environment using:

1) Standard microtiter plates.
2) Static incubation and ambient temperature and humidity

And to ascertain the gross morphology and phenotype of biofilms grown in the two models. An investigation of the development of semi-dry biofilms was undertaken when an attachment deficient mutant was used.

Materials and Methods

Preparation of dry biofilm models

Model 1 was prepared according to Almatroudi et al. (2015), but in a 24-well tissue culture plate format. Briefly the plates were incubated at 35^{o}C with agitation at 130rpm during batch phases and were dried at a high relative humidity (RH) of 66% at dehydration phases in a humidity chamber designed in the laboratory.

Model 2 was prepared as above, but with the following further modifications: 1) Plates were incubated at ambient temperature without agitation. 2) Plates were dried at ambient humidity during dehydration periods. Records of ambient humidity and temperature were kept with a thermo-hygrometer (Electronic Temperature Instrument Ltd, Worthing, England). The environmental average temperature and humidity values recorded during the experiment were 27.9±4.9^{o}C and 38.2±1.9%.

Preparation of test organisms

Three strains of *S. aureus* were used in the studies, two laboratory strains of clinical origin ATCC 25923 and NCTC 8178, and a sortase (*srt*A) mutant (*S. aureus* 1132), kindly gifted by Prof. Jose Penades (University of Glasgow). Strains were maintained in glycerol stocks at -80^{o}C, and cultured onto nutrient agar (Fisher Scientific, Leicestershire, United Kingdom) for each experiment.

A representative colony of each test organism was transferred into 10ml of Luria broth (Sigma Aldrich, St Louis, USA) and incubated at 37^{o}C at 150rpm for 24h. From the overnight culture, 1ml of bacterial suspension was transferred into a sterile 1.5ml Eppendorf tube and centrifuged at 5,590 x g for 5 min in a microcentrifuge. The harvested cells were washed twice with phosphate buffer saline (PBS), and the bacterial suspension adjusted by absorbance (OD_{570} = 0.2) to 10^9 colony forming units (CFU) ml^{-1}.

Evaluation of biomass formation and bacterial survival

The validation of the CDC DBM in flat bottomed microtiter plates was carried out using *S. aureus* ATCC 25923 and NCTC 8178. Test organisms were prepared at a final concentration of 1x10^8 CFU ml^{-1} in 5% tryptic soy broth (TSB) (Fisher Scientific, Leicestershire, United Kingdom) and 1ml was inoculated into each well of a tissue culture-treated 24-well flat-bottomed plate (Corning™ Costar™).

At 4, 7, 9 and 12 days, the biofilms were assayed for biomass formation and bacterial survival using crystal violet (CV) assay and colony forming units (CFU)/well counts, respectively. The percentage of coefficient of variation (%CV) for each well position was calculated using the obtained CFU ml^{-1} counts. The biofilm gross structure and composition were also determined by confocal laser scanning microscopy (CLSM) using fluorescent dyes. In addition, *S. aureus* 1132, a ΔsrtA mutant was also used in subsequent experiments for phenotypic analysis of biofilm formation and stress survival.

Crystal violet biomass estimation

Biomass estimation was adapted from that of Christensen et al. (1985). Briefly 1 ml of 0.1% w/v crystal violet was added onto biofilms washed with PBS, and left to stain for 30 min. Unbound dye was subsequently washed off carefully with distilled water and drained to

remove any residual unbound dye. The bound dye associated with the biofilm in each well was solubilized by adding 100% ethanol and incubated for 15min (Kim and Park 2013; Li et al. 2018). One hundred microlitre of the ethanol was transferred into fresh 96-well flat-bottom plates after carefully mixing by agitation and absorbance was then read at 570nm using a Tecan infinite f200 pro plate reader (Tecan, Grödig, Switzerland).

Enumeration of viable cells in the biofilms

The numbers of viable cells attached to the wells of the microtiter plates were determined by standard plate culture methodology with slight modifications (Sanders 2012). Each inoculated well was washed twice with PBS to remove unbound and loosely attached cells. One ml of PBS was then added to each well and the plates were sonicated in an ultrasonic bath (Fisher Scientific, Leicestershire, United Kingdom) for 5min (Kobayashi et al. 2009). To enhance removal of attached cells, the wells were scrapped carefully with the tip of 1ml pipette to fully remove all biomass. Recovered biomass was transferred into a 1.5ml Eppendorf tube and vigorously vortexed for 2min. This was followed by a sequential ten-fold serial dilution in PBS, and plating out on nutrient agar using the technique of Miles and Misra (Miles et al. 1938). The inoculated plates were incubated at 37^{o}C for 24h, after which the CFU/well was recorded and converted to $\log_{10}$ CFU/well values.

Evaluation of biofilm morphology and structure

The gross morphology and structure of 12h biofilms grown using Models 1 and 2 were evaluated by confocal laser scanning microscopy (CLSM). This methodology required a modification to the original protocol, in that 24-well plates were replaced by 6-well plates by the same manufacturer to allow space for the lens of the confocal microscope to reach the biofilms. 4.9ml of 1x10^{8} CFU ml^{-1} of *S. aureus* was dispensed into each well (in proportion to 1ml of the same concentration of cells used in the 24-well plates). The sequential periods of hydration batch phases and dehydration were identical as described in Table 1. After 12 days growth, biofilms were washed twice with PBS and stained with Molecular Probes™ LIVE/DEAD™ *Bac*Light™ Bacterial Viability Kit (Waltham, Massachusetts, United States), according to the manufacturer's instructions.

The samples were initially fixed with an equal volume of 5% TSB and 4% paraformaldehyde (Sigma-Aldrich Ltd, Dorset, UK), which was removed after 20 min and replaced with 4% paraformaldehyde for a further 20 min. Following removal of 4% paraformaldehyde, biofilms were hydrated with PBS for visualization using a Lecia SP5 confocal microscope (Leica Microsystems, Wetzlar, Germany) at x40 (numerical aperture 0.80) with a water immersion lens at an excitation wavelength of 488nm and an emission wavelength of 500 to 550nm. Each image was analysed in 3 different fields at random in the middle and at the edge of the plate and a representative field is shown. The depths of the biofilms were measured using Leica application suite (Advanced fluorescence lite 2.6.0 built 7266). The 3D images were constructed using icy for image analysis (Quantitative Image Analysis Unit, Paris, France).

Evaluation of biofilm composition

Biofilms aged 12 days in 6-well microtiter plates were washed twice with PBS and stained with the green fluorescent dye SYTO 9 and a protein stain, SyproOrange® (Molecular Probes, Invitrogen, USA). SYTO 9 was used to detect the attached bacterial cells, while SyproOrange was used to stain the proteins in the biofilm matrix. Both stains were prepared separately in the proportion of 1:1000ml in distilled water, and 1 ml of each was added to each well at the same time and the plates were incubated for 15 min in the dark at ambient temperature. The samples were fixed and viewed with confocal microscope as described above.

Assessing biofilm phenotype using antibiofilm effects of flucloxacillin

The antibiotic susceptibility profile of *S. aureus* ATCC 25923 and NCTC 8178 as biofilms grown under both sets of conditions and as planktonic cells were compared to confirm the multicellular behaviour of biofilms by increased antibiotic tolerance. Biofilms aged 12 days were washed twice with PBS to remove non-adherent cells. of Flucloxacillin (Sigma-aldrich, Dorset, UK) was prepared in TSB at different concentrations of 0.25, 0.5, 1.0, 100 and 1000µg mL^{-1} and each concentrations was added to the biofilms in the microtiter plate (Brady et al. 2017). From overnight cultures, 10µl of 1 x 10^9 cells ml^{-1} of each *S. aureus* strains were taken into 90µl of each antibiotic concentration in a non-treated round bottomed 96-well microtitre plates. Antibiotic-free inoculum were used as a positive control; antibiotic

and bacteria free wells media were used as negative control. The plates were incubated at 37^{o}C overnight in air and the lowest concentration that completely inhibited growth after 24h was defined as the MIC (Andrews 2001).

Statistical analysis

The quantity of biomass and $\log_{10}$ CFU/well formed in Models 1 and 2 by each strain of *S. aureus* used were compared using two-way ANOVA. The difference between the values obtained at different time points in each model was evaluated using one-way ANOVA. Graph production, data distribution, and statistical analysis were carried out using GraphPad Prism (version 6.07; San Diego, CA). As in CDC DBM, the assessment of the high throughput quality of the models in the microtiter plate was evaluated using the percentage of coefficient of variation (%CV) for each well position and the within run %.

Results

Model 1: Growth and biomass

The growth of *S. aureus* ATCCC 25923 as assessed by CV staining showed a fairly consistent amount of biomass between day 4 and day 12, with average biomass measured at OD_{570} of 0.36 and 0.33 respectively. *S. aureus* NCTC 8178 showed a two-fold increase in biomass between days 4 (0.19) and 6 (0.44) before reaching a maximum of 0.47 at day 12 ($p \leq 0.05$, $p \leq 0.01$). Although the biomass formed by the two strains of *S. aureus* were not significantly different at any time point as summarised in Figure 1a, more biomass was formed by *S. aureus* ATCCC 25923 on day 4 but on days 7,9 and 12 more biomass was obtained in *S. aureus* NCTC 8178. The average $\log_{10}$ CFU/well recovered from the formed biomass by standard plate count counts for *S. aureus* ATCC 25923 were constant from day 4 until day 12. *S. aureus* NCTC 8178 increased temporally between day 4 and day 12 ($p \leq 0.01$), with the average $\log_{10}$ CFU/well counts rising from 7.57 to 8.26. The CFU counts for the two strains of *S. aureus* were within the same log value not differing statistically except at day 4 when *S. aureus* ATCC 25923 was significantly higher than *S. aureus* NCTC 8178 ($p \leq 0.001$) as seen in Figure 1b.

Model 2: Growth and biomass

The CV assay used for quantification of biomass showed that the test isolates formed three-dimensional structure biomass that varied with the test isolates and growth periods. The average biomass of *S. aureus* ATCC 25923 measured at OD_{570} was highest at day 4 and fell by two-folds until day 12 from 1.64 to 0.69, respectively ($p \leq 0.001$). *S. aureus* NCTC 8178, followed a similar pattern with biomass declining between day 4 and day 9 ($p \leq 0.001$). However, by day 12 the biomass increased to 0.76 and was not significantly different from day 4, as summarised in Figure 2a. The number of viable cells recovered from the formed biomass by standard plate count showed a fairly constant number over the assessed time points. The average $\log_{10}$ CFU/well count for *S. aureus* ATCC 25923 was highest at day 4 (8.47) and declined to 7.59 on day 9 before increasing again to 7.75 at day 12 ($p \leq 0.05$, $p \leq 0.001$, $p \leq 0.0001$). The results of S. *aureus* NCTC 8178 were similar (Figure 2b).

As a measure of inter-assay variation for assessment of the high throughput quality of the models in the microtiter plate, the calculated coefficient of variation in the number of CFU

obtained from different wells of the microtiter plate at tested time points ranged from 1 to 6%.

Impact of model conditions on biomass production and survival

A comparison between the biomass yield and the number of viable cells that were recovered after the growth of *S. aureus* cells in the two models showed that the choice of model affected biofilm formation and minimal effect on survival of cells. *S. aureus* ATCC 25923 produced a significantly higher biomass in Model 2 compared with Model 1 at all time points. For *S. aureus* NCTC 8178 there was a significantly higher biomass in Model 2 at Day 4 and 12 ($p \leq 0.001$ and $p = 0.005$respectively) as illustrated in Figure 3a. When $\log_{10}$CFU/well counts were compared between both models the average $\log_{10}$CFU/well varied slightly in between the two models at the timepoints with values ranging from 7.09 to 8.42. However, there was no statistical difference was observed between the two models, except on day 4 for *S. aureus* NCTC 8178 ($p \leq 0.0001$) where higher counts were obtained in Model 2 (Figure 3b).

Impact of model conditions on biofilm structure

The CLSM images showed masses of predominantly viable cells attached to the walls of the microtitre plate. In both models, there were mixed colonies of dead and live cells attached to the surfaces in multilayers. In Model 1, the microcolonies were sparsely distributed across the plates with empty spaces in between the fluorescing aggregates of cells. The population of damaged cells as indicated by red fluorescent cells was low. The depths of *S. aureus* ATCC and NCTC 8178 biofilms were 8.02 and 9.30 µm, respectively (Figure 4). In Model 2, fluorescent images showed higher amount of attached biomass as indicated by the closely packed microcolonies of cells. Similar depths of 9.88 and 6.82 µm were obtained for *S. aureus* ATCC 25923 and NCTC 8178 biofilms in Model 2 (Figure 4). ECM characterisation of biofilms in Models 1 and 2 at 288h showed matrices of cells and extracellular polymers rich in protein content (Figure 5).

Impact of model conditions on stress tolerance

In order to establish any increased tolerance to antibiotics, flucloxacillin was used as opposed to a disinfectant to enabled detection of subtle changes in antimicrobial sensitivity. In the planktonic state, the MICs for *S. aureus* ATCC 25923 and NCTC 8178 were equivalent, 0.5 and 1.0 μg ml^{-1}, respectively. When these organisms were grown as biofilms in Model 1, the biofilms were more susceptible to flucloxacillin by a double fold for *S. aureus* ATCC 25923 and no difference was recorded for *S. aureus* NCTC 8178. However, when the organisms were grown in Model 2 the same value of 1.0 μg ml^{-1} was obtained for *S. aureus* NCTC 8178, while for *S. aureus* ATCC 25923 the MIC increased by 3 logs to >1000 μg ml^{-1}. The results are summarised in Table 2.

To further investigate this mechanism, the survival of Δ*srtA* mutant was evaluated in a semi-dry environment. Here it showed that *S. aureus* can survive with a deficient biofilm phenotype but may require ECM to maintain the integrity of the cells. The biomass values measured at OD_{570} obtained in Model 1 increased by three-fold between day 4 and day 12 from 0.09 to 0.24. In Model 2 the biomass measured at OD_{570} was highest at day 4 but declined by three-fold to day 12 from 1.45 to 0.42, respectively. Higher values of biomass were recorded in Model 2. The average biomass values and $\log_{10}$ CFU/well counts for the mutant and the wild types strains in Models 1 and 2 are summarised in Figures 1 and 2, respectively. Representative images are shown in Figure 6. Interestingly, when assessed for antimicrobial sensitivity as planktonic cells the MIC value of *S. aureus* Δ*srtA* mutant to flucloxacillin was 0.5μg ml^{-1}. However, as biofilms in Model 1 its MIC was 0.25 μg ml^{-1}, whereas in Model 2 the MIC was 10.0μg ml^{-1}, which is a 40-fold increment. The results are summarised in Table 2.

Discussion

Biofilms were introduced into the medical literature in 1985 (Costerton J 1985; Høiby N. et al. 2015; Høiby Niels 2017). Since then, there is an increasing number of scholarly articles being published on the subject biofilm, strengthening its acceptance in medicine and in other related fields of biological science. Many authors have come up with many methods for studying biofilms for thorough understanding of this evolving life of microbes. However, much of the research to date has been focused on wet, nutrient rich environments and may

not be fully representative of what is observed in the clinical environment. Recent work initially by Vickery et al. (2012) revealed that there are extensive biofilms found on "dry" surfaces in the healthcare environment and this has been confirmed by other studies (Hu et al. 2015; Ledwoch et al. 2018) . These biofilms are typically only a few microns thick, and this has catalysed the debate around what exactly constitutes a biofilm. Is this highly structured community hundreds of micrometres thick, or are these small bacterial aggregates exceeding 5 μm in diameter?

The primary aim of this study was to adapt the CDC DBM into a modular microtiter plate format to provide a high throughput, reproducible and cost-effective model for growing semi-dry biofilms. Results obtained demonstrate that. *S. aureus* attach and survive in microtiter plates under poor nutrition and intermittent dehydration, and that the biofilms formed in this study are similar to semi-hydrated biofilms grown in the CDC bioreactor both in terms of $\log_{10}$ CFU count and coefficient of variation between wells. There were however some differences. In Model 1, the average height of the biofilm was 8 - 9.3 μm compared with over 30 μm in the CDC bioreactor model. In addition, the biofilm in the CDC biofilm reactor covered the coupon surface compared with incomplete surface coverage in Model 1. The mean $\log_{10}$CFU/well for *S. aureus* ATCC 25923 and NCTC 8178 were 8.24 and 8.26 for the 2 laboratory strains- compared with the mean $\log_{10}$ CFU of 7.13 ± 0.04 in the original CDC bioreactor model (Almatroudi et al., 2015).

Model 2 was designed to closely model the conditions commonly encountered in healthcare settings in particular incubation without shaking under ambient conditions The level of humidity in this study was 38% compared with 66% in Almatroudi's paper but both could represent built environments in different parts of the world and indeed between different parts of buildings. The biofilms in Model 2 were again similar to both the original CDC DBM and Model 1 in terms of $\log_{10}$ CFU count (Almatroudi et al. 2015). Although the maximum depth of 9.88 μm measured in Model 2 was lower than 30 μm in CDC bioreactor model, Model 2 biofilms covered most of the microtiter plate surface as did biofilms on coupon surfaces in CDC bioreactor model. The biofilms grown with Model 2 at ambient conditions demonstrated the biofilm antibiotic tolerance feature which was not seen in biofilms grown under the engineered conditions of Model 1. In adapting a model in any study, it is important to mimic the conditions that closely resemble the case study; using different conditions in any study makes it difficult to interpret results in relationship to what obtains in nature and can

lead to wrong conclusions. The conditions maintained in Model 2 impacted positively on bacterial formation. Model 2 not only enhanced knowledge on bacterial survival in the environment but provides other advantages such as high throughput, requires minimal space to run many plates at a time and is easily affordable. The biofilms formed under the ambient conditions of the model were well attached, a feature that differentiates dry surface biofilms from wet biofilms (Almatroudi et al. 2015). It must be noted that while Model 2 may provide conditions that closely resemble the natural built environment, it is nearly impossible to accommodate all that happens in nature into a laboratory condition. The permutations of human traffic, microbial ecology, cleaning regime unique to every healthcare setting and all the environmental factors are expected to have a role on microbial ecology, survival and persistence.

In the investigation of the phenotype of the attached aggregates of cells, the physiological response of these aggregates of cells to stress validated the presence of biofilms. The ability of the *S. aureus* ATCC 25923 and NCTC 8178 to remain viable with most cell membranes intact after prolonged subjection to drying and poor nutrition suggests that the cells were not passively stuck to the plate surface as described for 'nonbiofilms' by Donlan Rodney M. and Costerton (2002) but there was a functional mechanism or barrier protecting the cells which was absent in the *S. aureus* 1132. This functional mechanism hypothetically may be biofilm formation/ the presence of protective extracellular polymers. This hypothesis was validated by the increased resistance of 12 days biofilms to antibiotics. Biofilm phenotypes are often characterised by several fold increase in resistance to antibiotics than their planktonic counterparts (Davies et al. 1998; Mah and O'Toole 2001; Balcázar et al. 2015) and this attribute is not always correlated by the size of the extracellular matrix of polymers. Qi et al. (2016) reported greater resistance in weak biofilm formers than in strong biofilm formers.

An important aspect of this study was the design and testing a model with conditions commonly encountered in healthcare settings such as incubation at ambient temperature without shaking. Although the resultant biofilms of this model were again comparable to both the original CDC DBM and Model 1 in terms both of $\log_{10}$ CFU count, higher biomass was recorded in Model 2 for all the test organism which could be due to the presence of more extracellular polymeric substances. The presence of excess ECM may have impacted on the demonstration of an antibiotic tolerance feature seen in Model 2 biofilms. Biofilms of *S. aureus* ATCC25923 grown with Model 1 conditions of high and steady incubation

temperature with agitation at batch phases exhibited increased antibacterial susceptibility when compared with the planktonic cells and this could possibly be due the environmental stress of dehydration and poor nutrition built into the dry biofilm model. The cell membranes were compromised, and the presence of little EPS left the cells vulnerable to antibiotics. Conversely the cells of *S. aureus* ATCC25923 in the biofilms grown with Model 2 although subjected to the same stress were protected probably due to the presence of more EPS. Although *S. aureus* NCTC 8178 exhibited a similar phenotype, its level of antibiotic tolerance was very low. The progressive accumulation of biomass in *S. aureus* NCTC 8178, may have allowed the cell membranes to become in some way damaged before they attained the biofilm phenotype leaving the cells vulnerable to antibiotics confirming that the ability of an organism to form ECM rapidly determines its reaction to environmental stressors (Grinberg et al., 2019).

In many previous studies (Donlan Rodney M. and Costerton 2002; Goeres et al. 2005; Hadi et al. 2010; Almatroudi et al. 2015), it has been postulated that shear is a necessary factor to the growth of robust biofilms and favours biofilm formation. Results from this study suggests that an absence to shear may be associated with increased adhesion and biofilm formation, however more work is needed to look at the effect of shear alone in Model 2 to clarify this. The biofilms formed in both Models 1and 2 were well attached, exhibiting continual attachment of cells despite sonication. Intermittent drying during the 12-day growth period may have been a contributing factor to this strong attachment but this is also the case in the clinic, where daily wetting, wiping, and drying of healthcare surfaces is the norm and the formation of adherent biofilms which persist on hospital surfaces despite routine cleaning and decontamination has been well described (Hu et al., 2015, Ledwoch et al., 2018). Although a starting inoculum of 9 log CFU ml^{-1} was used in this study, it is important to note that that this level of inoculum would be unlikely to happen often in the hospital environment (infected urine spills for example contain usually ≥ 5 log CFU ml^{-1} (Schmiemann et al. 2010)). This was however the inoculum size used in the CDC bioreactor model being replicated in this study. More work will be needed in the future with lower starting inocula to more closely mimic starting conditions found in the hospital environment.

The pattern of growth, survival and persistence of the sortase deficient mutant suggests that there may be other mechanisms than biofilm formation/ECM production by which *S. aureus*

survives in semi-dry environments. Not all microorganisms are able to form biofilms but, under unfavourable conditions may persist in dry environments as aggregates of microorganisms. These microbial aggregates have the potential for infection transmission or biofilm formation if favourable environmental conditions are met. These aggregates could be referred to biofilm-primed aggregates (BPA) (Kragh et al. 2016; Melaugh et al. 2016) . Bacteria may resist death in hostile environments in the following ways. In wet and nutrient rich environments organisms would persist in the form of biofilms cocooned in thick EPS (Donlan, 2002). In dry environments effective biofilm formers could persist in communities protected by thick (Almatroudi et al. 2015) or thin layers of EPS as described here for *S. aureus* ATCC 25923. The survival strategy for slow biofilm formers or non-biofilm formers could be as BPA, which may form EPS if favourable conditions return, as was observed in *S. aureus* NCTC 8178 or not as seen in *S. aureus* 1132 (Figure 7). Imaging of *S. aureus* sortase deficient mutant showed that the environmental stressors such nutrient and moisture deprivation had impacted on the integrity of the cells. These heavily compromised cells *S. aureus* sortase deficient mutant emphasise the role the enzyme plays in producing proteins needed for the protection of bacteria from stress and in the formation of biofilm (Guiton et al. 2009; Wang et al. 2019).

The role of dry biofilms in the spread of nosocomial infections may be underestimated. Biofilm persistence in the built environment could be more effectively studied if the right conditions and appropriate bacterial strains are used. Several studies on the link between wet biofilm and HAIs have been carried out but little or no attention has been paid on the impact stress in the dry environment has on the transfer and virulence of microorganism.

In conclusion, Models 1 and 2 are both relevant in the clinical setting. The numbers of bacteria obtained in Model 1 ($Log_{10}8.24$ - $Log_{10}8.26$/well) are within the inoculum densities of 10^8 to 10^9 required for planktonic cells in testing of hospital-grade disinfection (Anon 2009). Model 2 is a high throughput and low-cost dry biofilm model that allows the growth of biofilms with numbers ($Log_{10}7.8$/well) which is a reasonable representative of numbers of bacteria obtained from sampled surfaces ($Log_{10}7.2$ cm $^{-2}$) in the clinical environment (Almatroudi et al. 2016). It is also adaptable to the growth of biofilms under ambient conditions in any area of the world and not requiring the use of controlled temperature, humidity or shear. Model 2 could be used in further studies to understand why

microorganisms survive the healthcare environments and contribute to controlling the spread of healthcare associated infections.

Almatroudi A, Gosbell IB, Hu H, Jensen SO, Espedido BA, Tahir S, Glasbey TO, Legge P, Whiteley G, Deva A. 2016. Staphylococcus aureus dry-surface biofilms are not killed by sodium hypochlorite: implications for infection control. Journal of Hospital Infection. 93(3):263-270.
Almatroudi A, Hu H, Deva A, Gosbell IB, Jacombs A, Jensen SO, Whiteley G, Glasbey T, Vickery K. 2015. A new dry-surface biofilm model: an essential tool for efficacy testing of hospital surface decontamination procedures. Journal of microbiological methods. 117:171-176.
Andrews JM. 2001. Determination of minimum inhibitory concentrations. Journal of antimicrobial Chemotherapy. 48(suppl_1):5-16.
Anon. 2009. Therapeutic Goods Order No. 54 — Standard for Disinfectants and Sterilants, Canberra, Australian Government . Cited in Staphylococcus aureus dry-surface biofilms are not killed by sodium hypochlorite:implications for infection control. Journal of Hospital Infection, 93(3):263-270.
Arampatzi SI, Giannoglou G, Diza E. 2011. Biofilm formation: a complicated microbiological process. Aristotle University Medical Journal. 38(2):21-29.
Balcázar JL, Subirats J, Borrego CM. 2015. The role of biofilms as environmental reservoirs of antibiotic resistance. Frontiers in microbiology. 6:1216.
Brady AJ, Laverty G, Gilpin DF, Kearney P, Tunney M. 2017. Antibiotic susceptibility of planktonic-and biofilm-grown staphylococci isolated from implant-associated infections: should MBEC and nature of biofilm formation replace MIC? Journal of medical microbiology. 66(4):461-469.
Chowdhury D, Tahir S, Legge M, Hu H, Prvan T, Johani K, Whiteley GS, Glasbey TO, Deva AK, Vickery K. 2018. Transfer of dry surface biofilm in the healthcare environment: the role of healthcare workers' hands as vehicles. Journal of Hospital Infection. 100(3):e85-e90.
Christensen GD, Simpson W, Younger J, Baddour L, Barrett F, Melton D, Beachey E. 1985. Adherence of coagulase-negative staphylococci to plastic tissue culture plates: a quantitative model for the adherence of staphylococci to medical devices. Journal of clinical microbiology. 22(6):996-1006.
mCosterton J. 1985. Biomedical devices containing isothiazolones to control bacteria growth. Google Patents.
Costerton JW, Lewandowski Z, Caldwell DE, Korber DR, Lappin-Scott HM. 1995. Microbial biofilms. Annual Reviews in Microbiology. 49(1):711-745.
Davies DG, Parsek MR, Pearson JP, Iglewski BH, Costerton Jt, Greenberg E. 1998. The involvement of cell-to-cell signals in the development of a bacterial biofilm. Science. 280(5361):295-298.
Donlan RM. 2002. Biofilms: microbial life on surfaces. Emerg Infect Dis. 8(9).
Donlan RM, Costerton JW. 2002. Biofilms: survival mechanisms of clinically relevant microorganisms. Clinical microbiology reviews. 15(2):167-193.
Goeres DM, Loetterle LR, Hamilton MA, Murga R, Kirby DW, Donlan RM. 2005. Statistical assessment of a laboratory method for growing biofilms. Microbiology. 151(3):757-762.
Gomes LC, Deschamps J, Briandet R, Mergulhão FJ. 2018. Impact of modified diamond-like carbon coatings on the spatial organization and disinfection of mixed-biofilms composed of Escherichia coli and Pantoea agglomerans industrial isolates. International journal of food microbiology. 277:74-82.

Grinberg M, Orevi T, Kashtan N. 2019. Bacterial surface colonization, preferential attachment and fitness under periodic stress. PLoS computational biology. 15(3):e1006815.
Guiton PS, Hung CS, Kline KA, Roth R, Kau AL, Hayes E, Heuser J, Dodson KW, Caparon MG, Hultgren SJ. 2009. Contribution of autolysin and sortase A during Enterococcus faecalis DNA-dependent biofilm development. Infection and immunity. 77(9):3626-3638.
Hadi R, Vickery K, Deva A, Charlton T. 2010. Biofilm removal by medical device cleaners: comparison of two bioreactor detection assays. Journal of Hospital Infection. 74(2):160-167.
Hu H, Johani K, Gosbell IB, Jacombs ASW, Almatroudi A, Whiteley GS, Deva AK, Jensen S, Vickery K. 2015. Intensive care unit environmental surfaces are contaminated by multidrug-resistant bacteria in biofilms: combined results of conventional culture, pyrosequencing, scanning electron microscopy, and confocal laser microscopy. Journal of Hospital Infection. 91(1):35-44.
Høiby N. 2017. A short history of microbial biofilms and biofilm infections. Apmis. 125(4):272-275.
Høiby N, Bjarnsholt T, Givskov M, Molin S, Ciofu O. 2010. Antibiotic resistance of bacterial biofilms. International journal of antimicrobial agents. 35(4):322-332.
Høiby N, Bjarnsholt T, Moser C, Bassi GL, Coenye T, Donelli G, Hall-Stoodley L, Hola V, Imbert C, Kirketerp-Møller K. 2015. ESCMID⁎ guideline for the diagnosis and treatment of biofilm infections 2014. Clinical microbiology and infection. 21:S1-S25.
Kim H-S, Park H-D. 2013. Ginger extract inhibits biofilm formation by Pseudomonas aeruginosa PA14. PLoS One. 8(9):e76106.
Kobayashi H, Oethinger M, Tuohy MJ, Procop GW, Bauer TW. 2009. Improved detection of biofilm-formative bacteria by vortexing and sonication: a pilot study. Clinical orthopaedics and related research. 467(5):1360-1364.
Kostaki M, Chorianopoulos N, Braxou E, Nychas G-J, Giaouris E. 2012. Differential biofilm formation and chemical disinfection resistance of sessile cells of Listeria monocytogenes strains under mono-species and dual-species conditions with Salmonella enterica. Applied and environmental microbiology.AEM-07099.
Kragh KN, Hutchison JB, Melaugh G, Rodesney C, Roberts AE, Irie Y, Jensen PØ, Diggle SP, Allen RJ, Gordon V. 2016. Role of multicellular aggregates in biofilm formation. MBio. 7(2):e00237-00216.
Kritsotakis EI, Flora Kontopidou EA, Roumbelaki M, Ioannidou E, Gikas A. 2017. Prevalence, incidence burden, and clinical impact of healthcare-associated infections and antimicrobial resistance: a national prevalent cohort study in acute care hospitals in Greece. Infection and Drug Resistance. 10:317.
Ledwoch K, Dancer S, Otter J, Kerr K, Roposte D, Maillard J-Y. 2018. Beware Biofilm! Dry biofilms containing bacterial pathogens on multiple healthcare surfaces; a multicentre study. Journal of Hospital Infection.
Lei H, Jones RM, Li Y. 2017. Exploring surface cleaning strategies in hospital to prevent contact transmission of methicillin-resistant Staphylococcus aureus. BMC infectious diseases. 17(1):85.
Li B, Li X, Lin H, Zhou Y. 2018. Curcumin as a promising antibacterial agent: effects on metabolism and biofilm formation in S. mutans. BioMed research international. 2018.
Mah T-FC, O'Toole GA. 2001. Mechanisms of biofilm resistance to antimicrobial agents. Trends in microbiology. 9(1):34-39.
Melaugh G, Hutchison J, Kragh KN, Irie Y, Roberts A, Bjarnsholt T, Diggle SP, Gordon VD, Allen RJ. 2016. Shaping the growth behaviour of biofilms initiated from bacterial aggregates. PLoS One. 11(3):e0149683.
Miles AA, Misra SS, Irwin JO. 1938. The estimation of the bactericidal power of the blood. Epidemiology & Infection. 38(6):732-749.
Muazu A, Rahman NIA, Aliyu S, Abdullahi UF, Umar AF, Ogidi JA. 2017. Differential biofilm formation and chemical disinfection resistance of Escherichia coli on stainless steel and polystyrene tissue culture plate. International Journal of Research in Medical Sciences. 3(11):3300-3307.

Qi L, Li H, Zhang C, Liang B, Li J, Wang L, Du X, Liu X, Qiu S, Song H. 2016. Relationship between antibiotic resistance, biofilm formation, and biofilm-specific resistance in Acinetobacter baumannii. Frontiers in microbiology. 7:483.
Richmond GE, Evans LP, Anderson MJ, Wand ME, Bonney LC, Ivens A, Chua KL, Webber MA, Sutton JM, Peterson ML. 2016. The Acinetobacter baumannii two-component system AdeRS regulates genes required for multidrug efflux, biofilm formation, and virulence in a strain-specific manner. MBio. 7(2):e00430-00416.
Sanders ER. 2012. Aseptic laboratory techniques: plating methods. JoVE (Journal of Visualized Experiments).(63):e3064.
Schmiemann G, Kniehl E, Gebhardt K, Matejczyk MM, Hummers-Pradier E. 2010. The diagnosis of urinary tract infection: a systematic review. Deutsches Ärzteblatt International. 107(21):361.
Vickery K, Deva A, Jacombs A, Allan J, Valente P, Gosbell IB. 2012. Presence of biofilm containing viable multiresistant organisms despite terminal cleaning on clinical surfaces in an intensive care unit. Journal of Hospital Infection. 80(1):52-55.
Wang J, Shi Y, Jing S, Dong H, Wang D, Wang T. 2019. Astilbin Inhibits the Activity of Sortase A from Streptococcus mutans. Molecules. 24(3):465.

Table 1: Culture conditions for CDC DBM as developed by Almatroudi et al. (2015) and it consists of alternating cycles of dehydration and hydration at different time points from the start of incubation to the end. All experiments were undertaken in microtitre plates. Stages of wet (batch phase) and dry alternated for a cumulative total period of 12 days (288h).

Stage	Culture Condition	Cumulative growth hours (Days)
1	48 h batch phase in 5% TSB followed by 48 h dehydration	96h (4 days)
2	6 h batch phase in 5% TSB followed by 66 h dehydration	168h (7 days)
3	6 h batch phase in 5% TSB followed by 42 h dehydration	216h (9 days)
4	6 h batch phase in 5% TSB followed by 66 h dehydration	288h (12 days)

S. aureus strains	MIC range in µg ml^{-1}																				
	0.25			0.5			1.0			10.0			100.0			1000.0					
	P	M1	M2	P	M1	M2	P	M1	M2	P	M1	M2	P	M1	M2	P	M1	M2			
ATCC 25923	+	+	+	+	-	+	-	-	+	-	-	+	-	-	+	-	-	+			
NCTC 8178	+	+	+	+	+	+	+	+	+	-	-	-	-	-	-	-	-	-			
1132	+	+	+	-	+	-	-	+	-	-	+	-	-	-	-	-	-	-			

Table 2: Antibiotic susceptibility of 3 strains of *S. aureus* - ATCC 25923, NCTC 8178 and 1132 grown under different conditions to flucloxacillin.

Key: P= Planktonic; MI= Grown using Model 1, M2= Grown using Model 2, += Growth; - = No growth. *S. aureus* strains grown with Model 2 showed the highest resistance to flucloxacillin

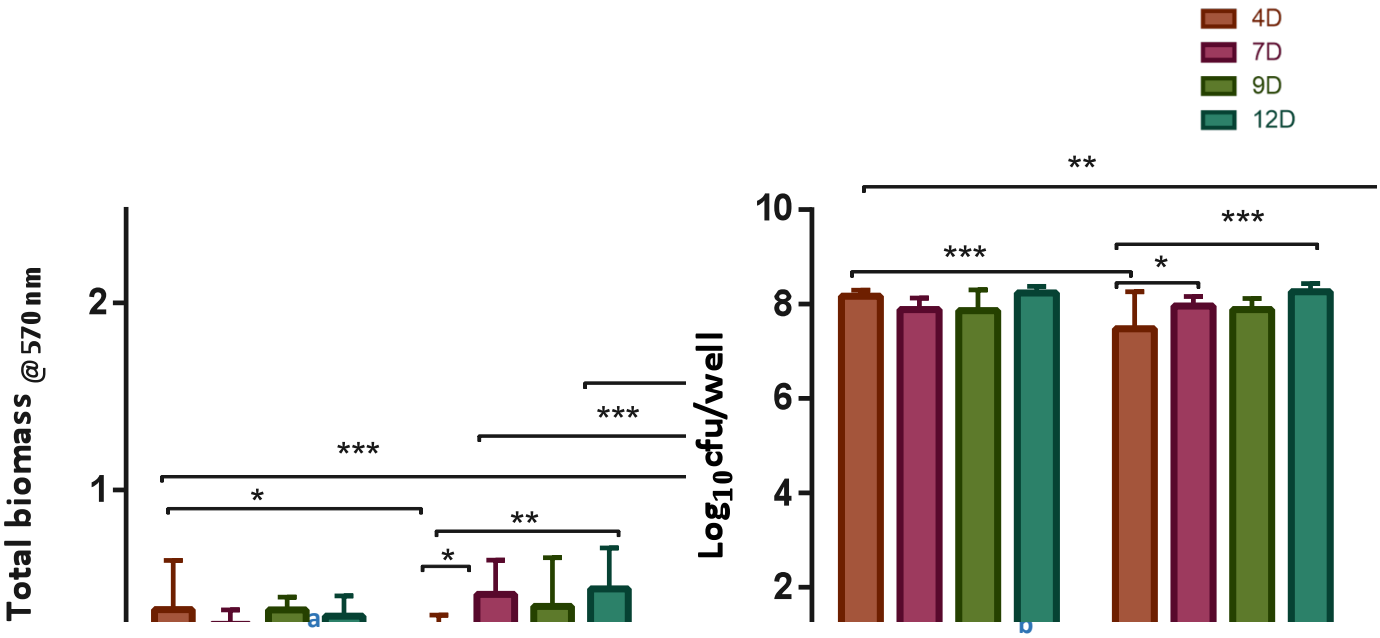

Figure 1: Representative biomass and log_{10} CFU/well of *S. aureus* ATCC 25923, NCTC 8178 and 1132 biofilms grown for defined time-points (4, 7, 9 and 12 days) using biofilm Model 1 as described in the materials and methods section. Overall biofilm biomass was determined using CV staining and is represented in Figure 1a, with biofilm composition quantified as a log_{10} CFU/well shown in Figure 1b (*=p≤0.05, **=p≤ 0.01 ***=p≤0.001). *S. aureus* ATCC 25923 achieved consistent average biomass from day 4 while for *S. aureus* NCTC 8178 its biomass was gradually built up over the test period. Log_{10} CFU/well obtained for *S. aureus* ATCC 25923 and NCTC 8178 were similar across the time points differing statistically only on day 4. Figure 1 also shows comparisons of the quantities of biomass obtained at different time points of 4, 7, 9 and 12 days for *S. aureus* ATCC 25923, NCTC 8178 and 1132 in Model 1, respectively (Figure 1a). Log_{10} CFU/well were compared in the same order in Figure 1b (*=p≤0.05, **=p≤ 0.01, ***=p≤0.001). The growth of *S. aureus* 1132 in terms of biomass and log_{10} CFU/well showed comparable growth characteristics between the ECM deficient mutant and the wild type strains. Key*: S. a = S. aureus,* D = Days

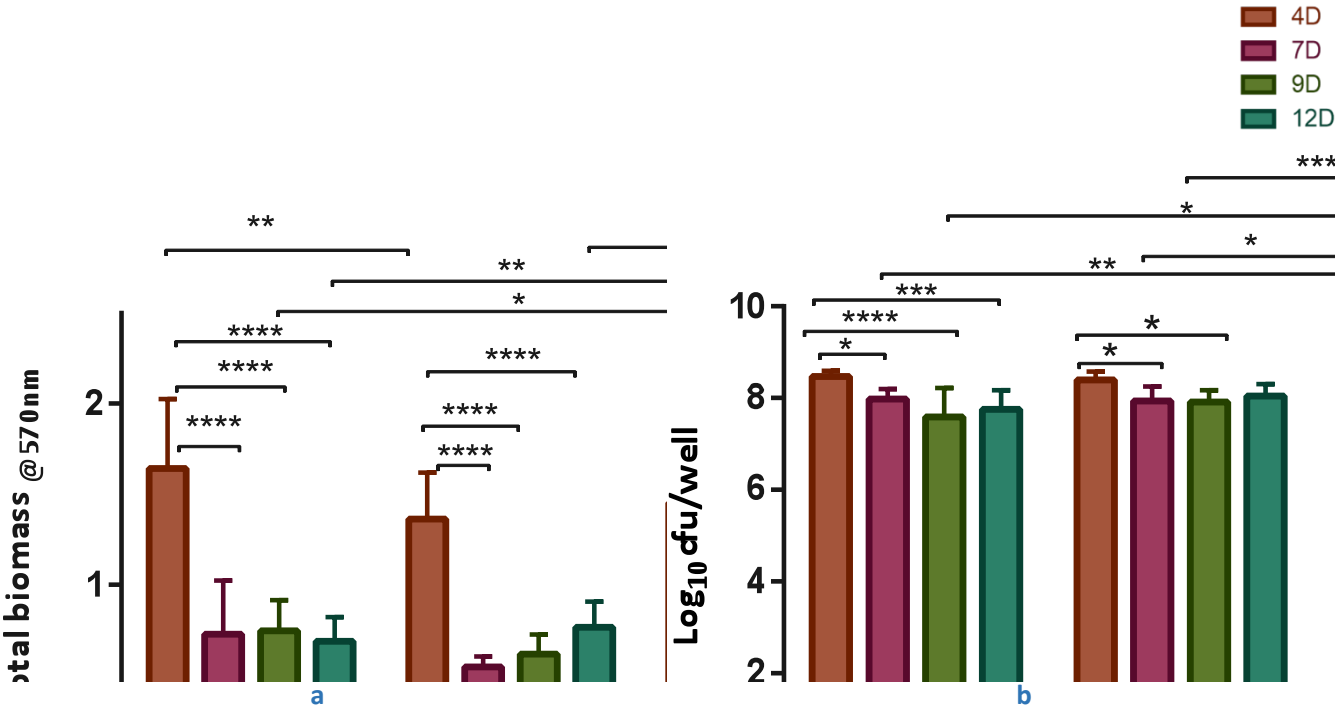

Figure 2: Representative biomass and log_{10} CFU/well of *S. aureus* ATCC 25923, NCTC 8178 and 1132 biofilms grown for defined time-points (4, 7, 9 and 12 days) using biofilm Model 2 as described in the materials and methods section. Overall biofilm biomass was determined using CV staining and is represented in Figure 2a, with biofilm composition quantified as a log_{10} CFU/well shown in Figure 2b (*=p≤0.05, , **=p≤ 0.01 , ***=p≤0.001, ****p≤0.0001). The average biomass harvest from *S. aureus* ATCC 25923 and NCTC 8178 were highest at day 4 which were followed by a decline. Log_{10} CFU/well was similar for the two test isolates. Figure 2 also shows comparisons of the quantities of biomass obtained at different time points of 4, 7, 9 and 12 days for *S. aureus* ATCC 25923, NCTC 8178 and 1132 in Model 2, respectively (Figure 2a). Log_{10} CFU/well were compared in the same order in Figure 2b (*=p≤0.05, **=p≤ 0.01, ***=p≤0.001, ****p≤0.0001). The growth of *S. aureus* 1132 in terms of biomass and log_{10} CFU/well showed comparable growth characteristics between the ECM deficient mutant and the wild type strains. Key*: S. a = S. aureus,* D = Days

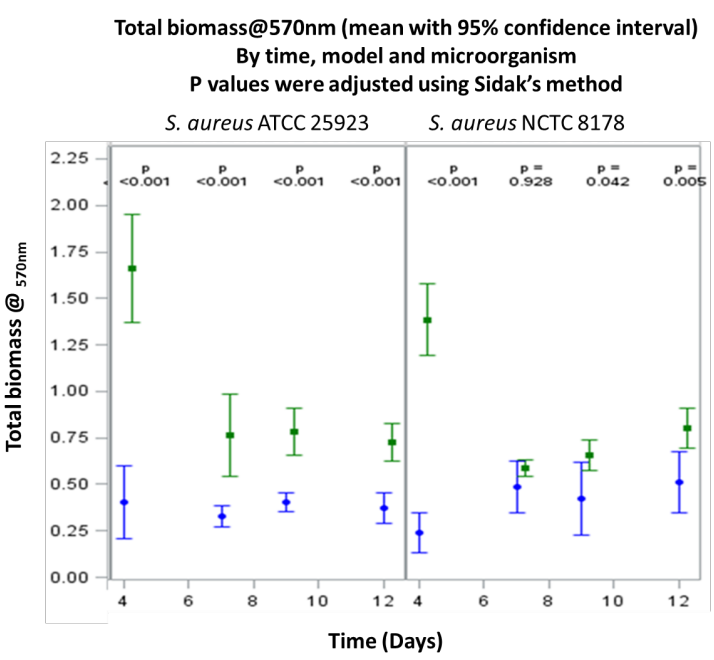

a

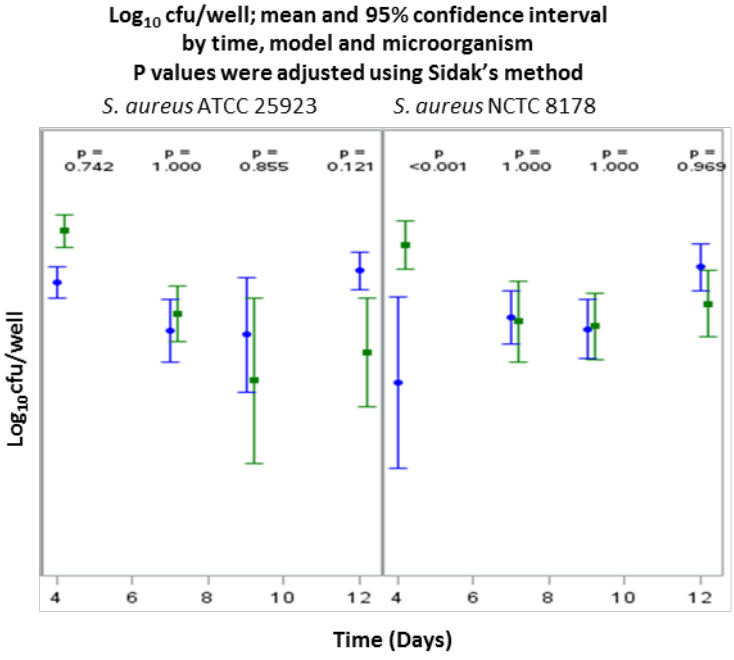

b

Figure 3: Comparisons of the quantities of biomass/well and the $\log_{10}$ CFU/well obtained for *S. aureus* ATCC 25923 and NCTC 8178 at different time points of 4, 7, 9 and 12 days in Models 1 and 2 (Figures 3a and b respectively). More biomass was harvested in Model 2 than in Model 1 for the two strains. The $\log_{10}$ CFU/ml from the two models were equal except day 4 for *S. aureus* NCTC 8178 where higher counts were seen in Model 2. Key: = Model 1, = Model 2

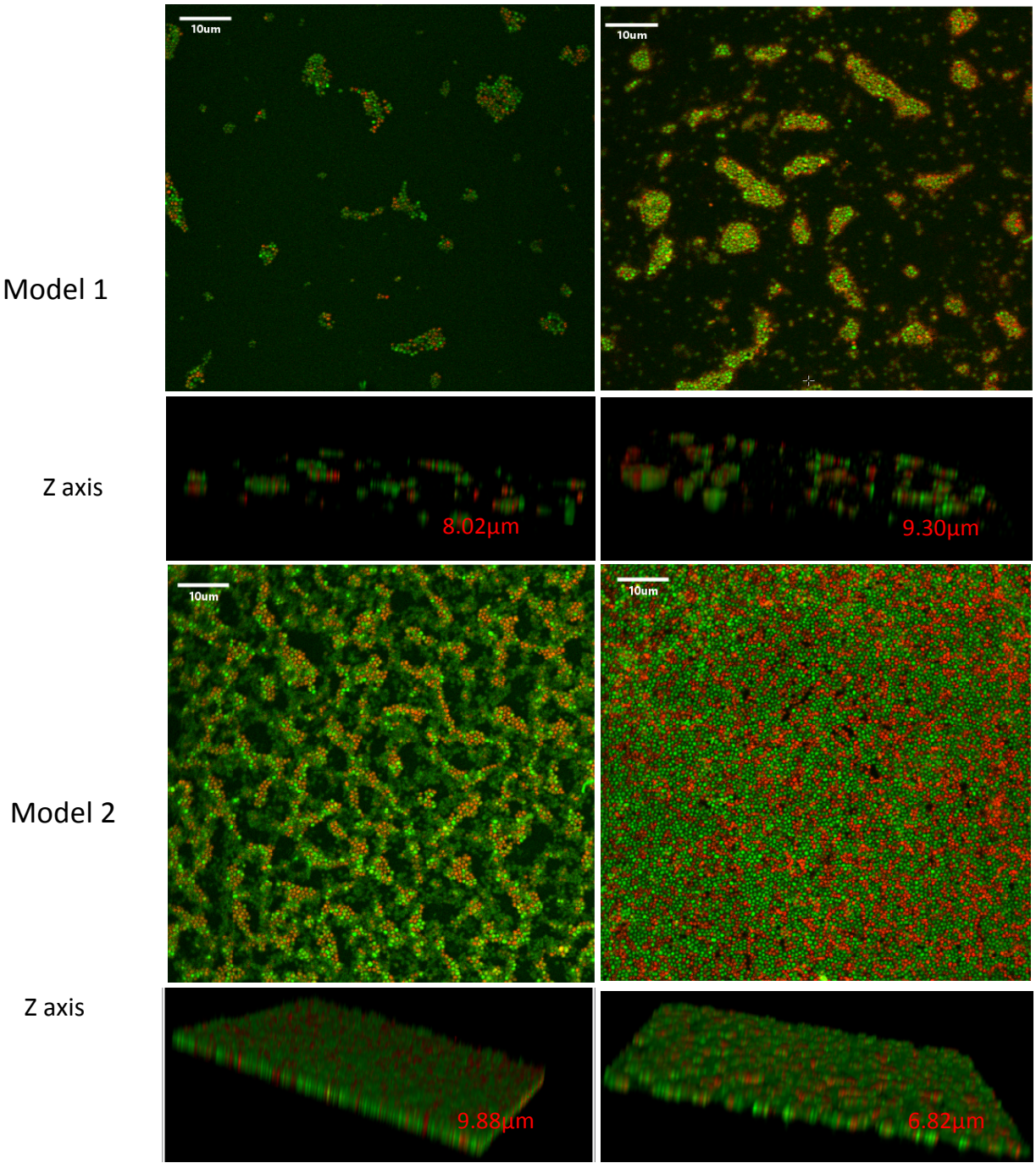
Model 1
Z axis
Model 2
Z axis
10um
10um
10um
10um
8.02µm
9.30µm
9.88µm
6.82µm
S. aureus ATCC 25923 [24]
S. aureus NCTC 8178
i
ii

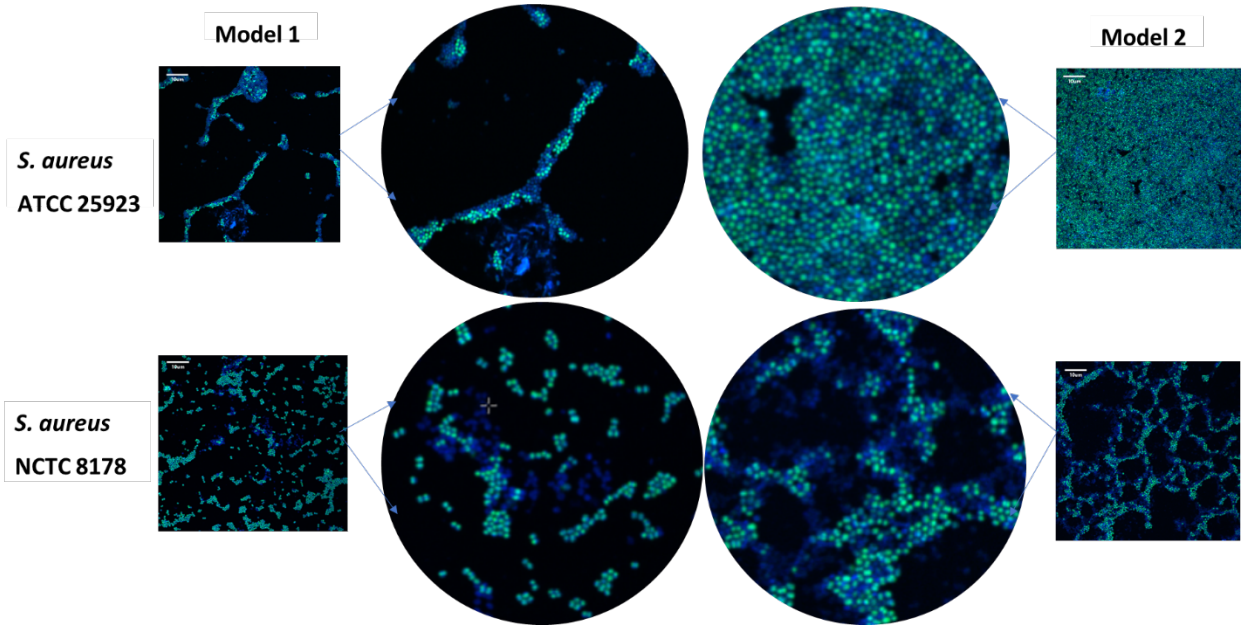

Figure 5: The biofilms as stained with a mixture of sypro orange (a protein-dye) and the DNA stain syto09 to show ECM composition. This showed matrices of extracellular polymers rich in protein content (presented in blue colour) from 12 days old cultures of *S. aureus* ATCC 25923 and NCTC 8178 grown using Models 1 and 2.

Three fields were viewed at random in the middle and at the edge of the plate and a representative field is shown here. Fluorescence was captured with a × 40 (numerical aperture 0.80) water-immersion lens at an excitation wavelength of 488nm and an emission wavelength of 500 to 550nm. Magnification = x400, Scale = 10 µm

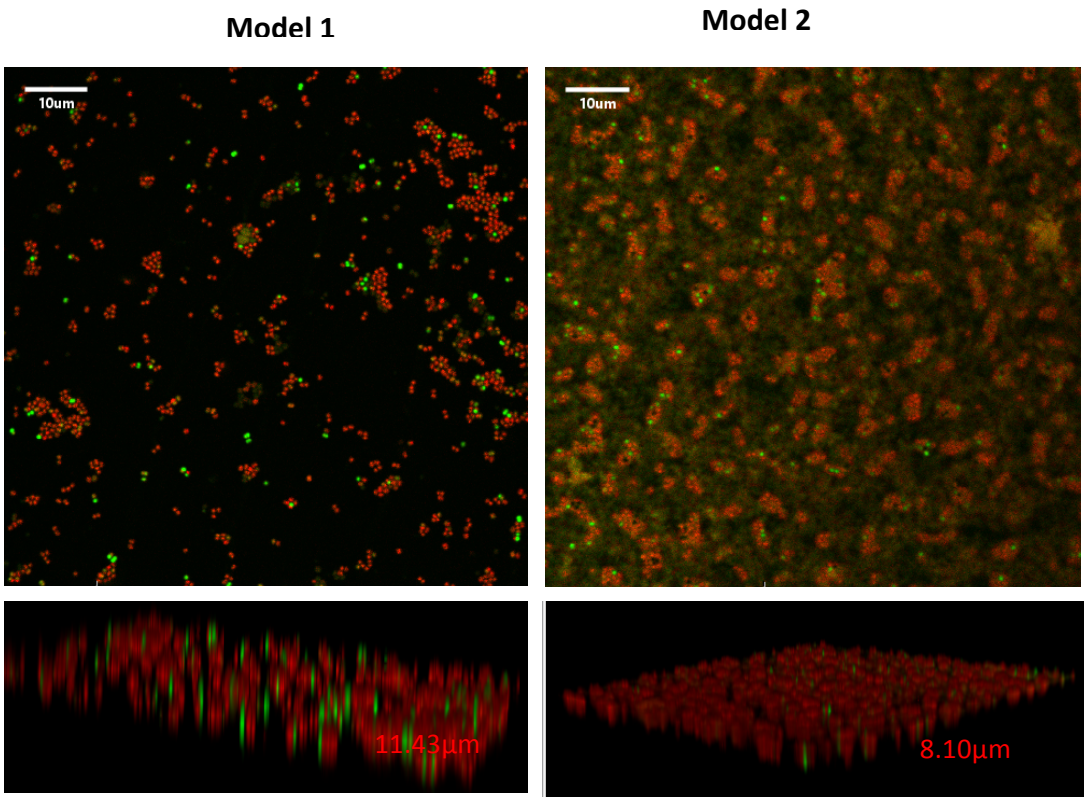

Figure 6: The biofilm gross structures of *S. aureus* 1132 grown using models 1 and 2 at 12 days as seen under CLSM when stained with live dead stain. Its biomass was in multilayers of cells which were mainly damaged in the two models. The cell matrix depths were 11.43 and 8.1µm in Models 1 and 2 respectively (Key*: S. a* = *S. aureus,* D = Days). Magnification = x400, Scale = 10 µm

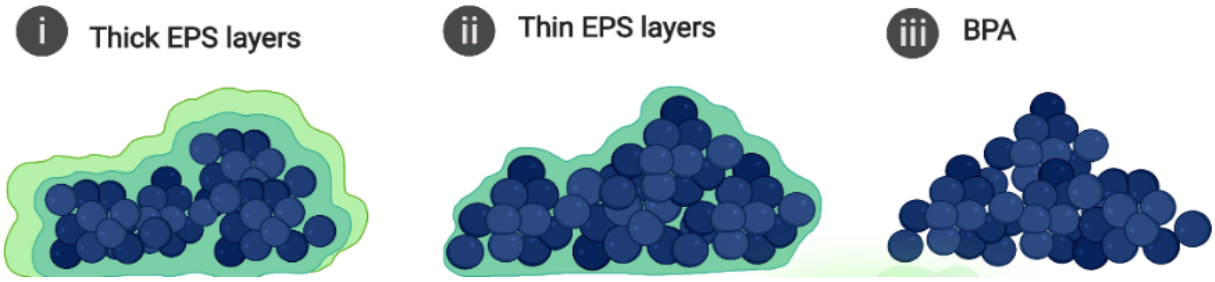

Figure 7: The possible modes by which bacterial cells can survive on semi-dry surfaces are shown here. In semi-dry environments, good biofilm formers could persist in communities protected by thick EPS as described by Almatroudi et al. (2015) or thin layers of EPS as described for *S. aureus* ATCC 25923 in this study (i & ii). The survival strategy for slow biofilm formers or non-biofilm formers could be as BPA (Kragh et al., 2016, Melaugh et al., 2016), which may form EPS if favourable conditions return as was observed in *S. aureus* NCTC 8178 (ii & iii) or may not as seen in *S. aureus* 1132 (iii).